

Species-dependent ion escape on Titan

Fa-Yu Jiang^{1,2}, Jun Cui^{2,3,4*}, Ji-Yao Xu¹, and Yong Wei⁵

¹State Key Laboratory of Space Weather, National Space Science Center, Chinese Academy of Sciences, Beijing 100190, China;

²Key Laboratory of Lunar and Deep Space Exploration, National Astronomical Observatories, Chinese Academy of Sciences, Beijing 100101, China;

³School of Atmospheric Sciences, Sun Yat-sen University, Zhuhai, Guangdong 519082, China;

⁴Chinese Academy of Sciences Center for Excellence in Comparative Planetology, Hefei 230026, China;

⁵Key Laboratory of Earth and Planetary Physics, Institute of Geology and Geophysics, Chinese Academy of Sciences, Beijing 100029, China

Abstract: Cassini observations over the past ten years have revealed that Titan possesses a chemically complex ionosphere. In this study, we investigate the relative contributions of different ion species to the total ion escape on Titan, by dividing all ion species probed by the Cassini Ion Neutral Mass Spectrometer (INMS) into six groups according to their mass-to-charge ratios (M/Z). For the three lightest ion groups, with characteristic M/Z of 22, 41, and 52 daltons, the observed scale heights tend to be lower than the scale heights predicted by assuming diffusive equilibrium; for the three heavier groups, observed and predicted scale heights are in general agreement, implying that most ion escape from Titan is by relatively light species, with $M/Z < 60$ daltons. A diffusion model is constructed to describe the density distribution of each ion group in regions where the effect of ionospheric chemistry could be neglected. The data model comparison predicts an optimal total ion escape rate of $3.1 \times 10^{24} \text{ s}^{-1}$, of which more than 99% is contributed by relatively light ions with $M/Z < 32$ daltons.

Keywords: Titan; planetary ionospheres; atmospheric escape

Citation: Jiang, F. -Y., Cui, J., Xu, J. -Y., and Wei, Y. (2019). Species-dependent ion escape on Titan. *Earth Planet. Phys.*, 3(3), 183–189. <http://doi.org/10.26464/epp2019020>

1. Introduction

The presence of a substantial ionosphere on Titan was first revealed by the Voyager-1 radio occultation measurements (Bird et al., 1997). Multi-instrumental observations made by the Cassini spacecraft during its encounters with Titan further indicated that the ionosphere on Titan was chemically complex (e.g., Wahlund et al., 2005; Cravens et al., 2005, 2006; Vuitton et al., 2007), populated mainly by HCNH^+ and C_2H_5^+ but also with a substantial inventory of other species (Cravens et al., 2006).

Subsequent studies have revealed substantial escape of ions from Titan. Based on Cassini Radio and Plasma Wave Science (RPWS) data acquired during the first two Titan flybys, Wahlund et al. (2005) estimated a total ion escape rate of $\sim 10^{25} \text{ s}^{-1}$, which is higher than the value of $\sim 5 \times 10^{24} \text{ s}^{-1}$ predicted by global multispecies Magnetohydrodynamic (MHD) models (e.g., Ma YJ et al., 2006) but lower than the value of $\sim (1.5\text{--}6) \times 10^{25} \text{ s}^{-1}$ predicted by hybrid models (e.g., Sillanpää et al., 2006; Modolo and Chanteur, 2008). By comparing the measured RPWS electron density distribution with that in diffusive equilibrium, Cui J et al. (2010) obtained a comparable total ion escape rate of $\sim (1.7 \pm 0.4) \times 10^{25} \text{ s}^{-1}$. For comparison, the neutral escape rate of $\sim 10^{27} \text{ s}^{-1}$, primarily contributed by escaping H_2 molecules (e.g., Cui J et al., 2008, 2011; Strobel,

2010; Tucker et al., 2013), is significantly higher than the ion escape rate on Titan.

Information on the escape rates of a restricted set of ion species is also available from Cassini data collected during several individual Titan flybys. Using Cassini Plasma Spectrometer (CAPS) data, Sittler et al. (2010) estimated an ionospheric H^+ and H_2^+ escape rate of $\sim 4 \times 10^{24} \text{ s}^{-1}$ for the T9 flyby. Investigations by Coates et al. (2012) based on CAPS data revealed both heavy (with mass-to-charge ratio, $M/Z = 16$ and 28 Da (Dalton)) and light ($M/Z = 1\text{--}2$ Da) ion populations streaming into the magnetic tail region of Titan. These authors estimated the escape rates of ion species with $M/Z = [1\text{--}2, 16, \text{ and } 28]$ Da to be $[0.1, 1.4, \text{ and } 1.4] \times 10^{24} \text{ s}^{-1}$ for T9, $[0.2, 0.5, \text{ and } 0.5] \times 10^{24} \text{ s}^{-1}$ for T63, and $[0.1, 0.2, \text{ and } 0.2] \times 10^{24} \text{ s}^{-1}$ for T75. Based on Cassini Ion and Neutral Mass Spectrometer (INMS) data acquired during the T40 flyby, Westlake et al. (2012) found an extended distribution of CH_5^+ , HCNH^+ , and C_2H_5^+ over the altitude range from 2225 to 3034 km, and estimated a representative ion outflow velocity of $0.8\text{--}1.5 \text{ km}\cdot\text{s}^{-1}$, equivalent to an ion escape rate of $\sim 10^{24} \text{ s}^{-1}$ for each of these species. These authors suggested that the observed ions were created below the exobase, followed by upward transport driven by both thermal pressure and magnetic pressure. More recently, Romanelli et al. (2014) analyzed the ionospheric flux flowing away from Titan based on the CAPS measurements made during T17, T19, and T40. They computed the relative abundances and escape rates of two main groups of ions with M/Z ranging from 15 to 17 Da and from 28 to 31 Da, and obtained the respective ion escape rates of

Correspondence to: J. Cui, cuijun7@mail.sysu.edu.cn

Received 05 DEC 2018; Accepted 14 MAR 2019.

Accepted article online 01 APR 2019.

©2019 by Earth and Planetary Physics.

$(1.1\text{--}1.3) \times 10^{25} \text{ s}^{-1}$ for T17, $(0.7\text{--}1.2) \times 10^{25} \text{ s}^{-1}$ for T19, and $(3.2\text{--}6.5) \times 10^{24} \text{ s}^{-1}$ for T40. In this study, we investigate further the relative contributions of different ion species to the total ion escape on Titan in a globally averaged sense, by dividing all the ion species up to $M/Z \sim 99$ Da sampled by the INMS into six groups according to their M/Z values.

The layout of the paper is as follows: A brief description of the INMS observations is presented in Section 2. The implication of these observations is the topic of Section 3 where we use a diffusion model to describe the density distribution of each ion group and derive the respective escape rate. Finally, we summarize and discuss our results in Section 4.

2. Observations

The data used in our analysis relies exclusively on the globally averaged Cassini INMS measurements obtained during 19 close encounters of Cassini with Titan, known in project parlance as T5, T17, T18, T26, T32, T36, T39, T40, T48, T50, T51, T57, T59, T61, T65, T71, T83, T84, and T86, for which the ion density data are available in the Open Source Ion (OSI) mode (Waite et al., 2004). The ion densities are retrieved based on the algorithm described in Mandt et al. (2012). The electron number densities and temperatures are obtained from the RPWS Langmuir probe (LP) measurements also made onboard Cassini (Gurnett et al., 2004). The geometrical information of the 19 Titan flybys considered here is de-

tailed in Table 1, including the date of observation, the latitude (LAT), the longitude (LON), the solar zenith angle (SZA), as well as the 10.7 cm solar radio index ($F_{10.7}$) at 1 AU in solar flux unit (SFU, $10^{-19} \text{ erg}\cdot\text{cm}^{-2}\cdot\text{s}^{-1}\cdot\text{Hz}^{-1}$), whereas LAT, LON, and SZA refer to the closest approach (CA). The table reveals that the Cassini dataset used here samples near evenly the dayside and the nightside, the ramside and the wakeside, as well as the full latitude range of Titan, with the maximum available $F_{10.7}$ index up to 140. Accordingly, our sample represents reasonably the globally averaged situation of Titan under low to mid solar activity conditions.

The ion species with $M/Z < 100$ sampled by the INMS are divided into six ion groups (G1–G6) according to their M/Z values, as listed in Table 2. For each group, we assign a representative group mass by the respective median M/Z value, denoted as $\langle M/Z \rangle$. These masses are later used to determine the density scale heights and escape rates of various ion groups.

The globally averaged ion density profiles for the six ion groups measured by the INMS are presented in Figure 1 with distinct colors. As shown in the figure, ion group G1 with a M/Z range of 12 to 31 Da is the most abundant population, with densities comparable to the electron densities at all altitudes. But it is important to note that because of the presence of both negative ions and positive ions heavier than $M/Z = 100$ Da (e.g., Wahlund et al., 2009; Coates et al., 2007, 2009), the total ion densities are not always identical to the electron densities. For simplicity, we treat the

Table 1. Geometry for each flyby in our sample^a

Flyby	Date	LAT	LON	SZA	$F_{10.7}$
T5	16/04/2005	74°N	271°	127°	84
T17	07/09/2006	23°N	57°	44°	88
T18	23/09/2006	71°N	357°	90°	71
T26	10/03/2007	32°N	358°	149°	70
T32	13/06/2007	84°N	2°	107°	73
T36	02/10/2007	60°S	109°	67°	67
T39	20/12/2007	70°S	177°	61°	70
T40	05/01/2008	12°S	130°	38°	77
T48	05/12/2008	10°S	179°	25°	67
T50	07/02/2009	34°S	306°	136°	69
T51	27/03/2009	30°S	235°	84°	71
T57	22/06/2009	42°S	178°	128°	70
T59	24/07/2009	62°S	179°	112°	71
T61	25/08/2009	20°S	237°	86°	69
T65	12/01/2010	82°S	358°	95°	90
T71	07/07/2010	56°S	303°	82°	77
T83	22/05/2012	73°N	128°	71°	124
T84	07/06/2012	39°N	283°	75°	132
T86	26/09/2012	63°N	201°	47°	140

Notes: ^aVarious columns, from left to right, give the flyby name, the date of observation, the latitude (LAT), the longitude (LON), and the solar zenith angle (SZA), all referred to the closest approach (CA), as well as the corresponding 10.7 cm solar radio index at 1 AU in solar flux unit (SFU, i.e., $10^{-19} \text{ erg}\cdot\text{cm}^{-2}\cdot\text{s}^{-1}\cdot\text{Hz}^{-1}$).

Table 2. Six ion groups divided according to their M/Z values and their escape rates

Ion group	$\langle M/Z \rangle$	M/Z	Typical species ^a	Escape rate (s ⁻¹)
G1	22	12–31	CH ₃ ⁺ , CH ₄ ⁺ , CH ₅ ⁺ , NH ₄ ⁺ , HCNH ⁺ , C ₂ H ₅ ⁺ , CH ₂ NH ₂ ⁺	3.1×10 ²⁴
G2	41	36–45	CHCN ⁺ , C ₃ H ₃ ⁺ , C ₃ H ₄ ⁺ , C ₃ H ₅ ⁺ , CH ₃ CNH ⁺ , C ₃ H ₇ ⁺	1.7×10 ²²
G3	52	49–57	C ₄ H ₃ ⁺ , HC ₃ NH ⁺ , C ₄ H ₅ ⁺ , C ₂ H ₃ CNH ⁺ , C ₄ H ₇ ⁺ , C ₂ H ₅ CNH ⁺	3.4×10 ²¹
G4	66	61–69	C ₅ H ₅ ⁺ , C ₄ H ₃ NH ⁺ , C ₅ H ₇ ⁺ , C ₄ H ₅ NH ⁺ , C ₅ H ₉ ⁺	D. E. ^b
G5	79	73–80	C ₆ H ₃ ⁺ , HC ₅ NH ⁺ , C ₆ H ₅ ⁺ , C ₅ H ₃ NH ⁺ , C ₆ H ₇ ⁺ , C ₅ H ₅ NH ⁺	D. E.
G6	91	84–94	C ₇ H ₅ ⁺ , C ₆ H ₃ NH ⁺ , C ₇ H ₇ ⁺ , C ₆ H ₅ NH ⁺ , C ₇ H ₉ ⁺ , C ₆ H ₇ NH ⁺	D. E.

Notes: ^aA more detailed list of Titan's ionospheric species can be found in Table 2 of Vuitton et al. (2007). ^bD. E. stands for diffusive equilibrium.

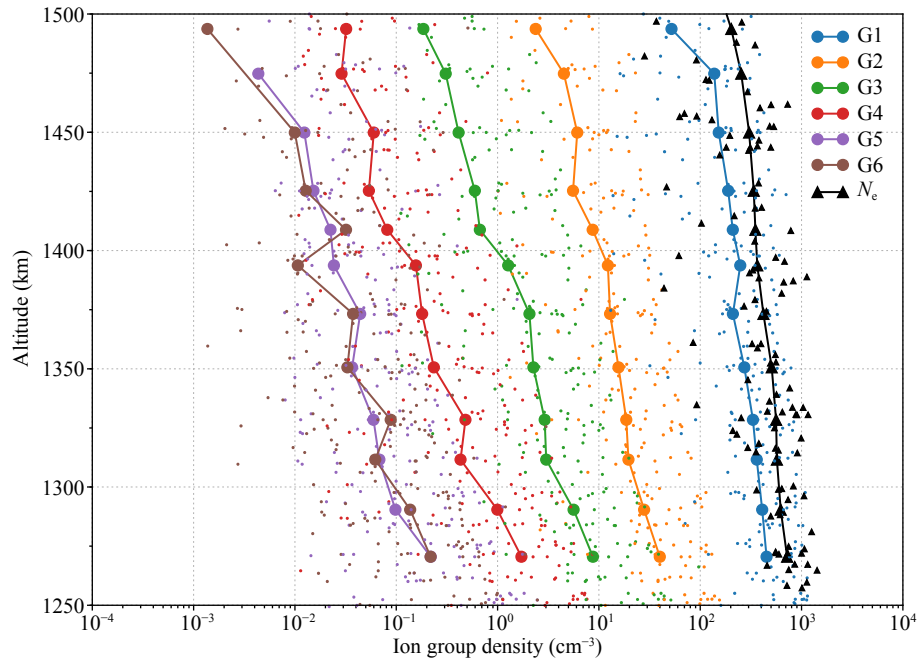


Figure 1. The INMS density profiles of the six ion groups (small colored dots) with $M/Z < 100$ divided according to their M/Z values (see Table 1 for details) sampled during the 19 Titan flybys considered in this study, as well as the respective electron density profile (black triangles) extracted from the RPWS LP measurements. The solid lines show the globally averaged profiles with a vertical resolution of 20 km.

most abundant ion group as one single major ion species, and regard the other five ion groups as minor ion species. Clues to the implications of the INMS density profiles could be gained with the aid of the momentum equation in the diffusion approximation, neglecting all ionospheric chemical terms. The lower boundary is placed at 1250 km to ensure that the regions examined here lie above the photochemical equilibrium region (e.g., Ma YJ et al., 2006; Cui J et al., 2010), while the upper boundary is placed at 1500 km to ensure that accurate density determination could be achieved for each of the ion groups listed in Table 1 (e.g., Cui J et al., 2009, 2010; Mandt et al., 2012). Note that although the ions lighter than $M/Z = 40$ Da manifest as two separate ion groups in a typical INMS ion mass spectrum and were divided into two mass groups by Ma YJ et al. (2006), in this study we do not distinguish between these two groups, which greatly simplifies the analysis presented below.

3. Species-Dependent Ion Escape

In the diffusion approximation, the momentum equation in the

vertical direction for the major ions and electrons in Titan's partially ionized atmosphere can be expressed as (Schunk and Nagy, 2009)

$$\nabla p_i - n_i e \mathbf{E} - n_i m_i \mathbf{G} = n_i m_i \nu_{in} (\mathbf{u}_n - \mathbf{u}_i), \quad (1)$$

$$\nabla p_e + n_e e \mathbf{E} = 0, \quad (2)$$

where p_i , n_i , and m_i are the pressure, number density, and mass of the major ion species i , p_e and n_e are the pressure and number density of electrons, e is the electron charge, \mathbf{E} is the ambipolar electric field, \mathbf{G} is the local gravity, \mathbf{u}_i and \mathbf{u}_n are the major ion and neutral drift velocities, and ν_{in} is the ion-neutral momentum transfer collision frequency. For the minor ion species l , the Coulomb collisions with the major ion species i should also be considered in the momentum equation, written as (Schunk and Nagy, 2009)

$$\nabla p_l - n_l e \mathbf{E} - n_l m_l \mathbf{G} = n_l m_l [\nu_{ln} (\mathbf{u}_n - \mathbf{u}_l) + \nu_{li} (\mathbf{u}_i - \mathbf{u}_l)], \quad (3)$$

where ν_{li} is the ion-ion momentum transfer collision frequency. The stress tensor term is neglected in the momentum equations because it is significantly smaller than the plasma pressure gradi-

ent and gravitational terms (e.g., Schunk and Nagy, 2009; Cui J et al., 2010). In addition, all terms in the electron momentum equation that are proportional to the electron mass have been dropped out owing to the small electron mass. The vertical drift velocity of the neutral background gas is also neglected for simplicity (e.g., Müller-Wodarg et al., 2008). Finally, in the globally averaged sense, the magnetic pressure term is also much smaller than both the thermal plasma pressure term and the gravitational term by two orders of magnitude over the altitude range considered here (see their Fig. 2). Therefore, we ignore for simplicity the contribution of the ambient magnetic field in this study. However, we caution that on the nightside of Titan, the magnetic pressure force is likely important, as noted by Cui J et al. (2010) and Cravens et al. (2010). Since ion escape is stronger on the dayside as compared to the nightside, such an approximation should not influence our derived ion escape rates.

Following Schunk and Nagy (2009), the ion-neutral momentum transfer collision frequency can be calculated with

$$v_{in} = 2.21\pi \frac{n_n m_n}{m_i + m_n} \sqrt{\frac{\gamma_n e^2}{\mu_{in}}}, \quad (4)$$

where n_n and m_n are the neutral number density and molecular mass, γ_n is the neutral gas polarizability, and μ_{in} is the reduced mass defined as $\mu_{in} = m_i m_n / (m_i + m_n)$. The ion-ion momentum transfer collision frequency is obtained with

$$v_{ii} = 1.27 \frac{Z_l^2 Z_i^2 M_{li}^{1/2}}{M_l} \frac{n_i}{T_i^{3/2}}, \quad (5)$$

where Z_l and Z_i are the ion charge numbers, M_{li} is the reduced mass in Dalton, M_l is the minor ion mass in Dalton, and T_i is the ion temperature assumed to be common for all ion species.

The INMS ion density scale heights at 1250–1500 km, along with uncertainties, are displayed by the open squares in Figure 2 as a function of the ion group mass. To interpret the observations, we start with the assumption that all species of Titan’s ionosphere are under D. E., predicting the ion density scale height to be $H_{DE} = \frac{2k_b T_i}{m_i g}$ for the major ion species i and $H_{DE} = \frac{k_b T_i}{(m_l - m_i/2)g}$ for each of the minor ion species l , where k_b is the Boltzmann constant (Schunk and Nagy, 2009). The ion density scale height under D. E. as a function of mass is displayed in Figure 2 for two representative ion temperatures of 250 K (red) and 150 K (blue). These values essentially encompass the ion temperature measurements made by the Cassini CAPS Ion Beam Sensor (IBS) at altitudes of our interest (Crary et al., 2009). For the ion temperature of 250 K, Figure 2 reveals that the scale heights under D. E. for ion groups lighter than 60 Da are substantially higher than the corresponding INMS scale heights, indicating that the three lightest ion groups G1–G3 experience considerable escape on Titan. In contrast, the agreement between the observed and predicted scale heights within measurement uncertainties for ion groups G4–G6 implies that relatively heavy ions are approximately under D. E. in the globally averaged sense. For the reduced ion temperature of 150 K, only the lightest ion group G1 suffers significant escape, whereas the data suggest a net inflow of ions heavier than 30 Da. Such a scenario is clearly unrealistic since no external sources of such heavy ions can be identified in the Saturnian system and the local production of heavy ions in Titan’s upper atmosphere is mainly at altitudes below 1250 km (e.g., Vuitton et al., 2007; De La Haye et al., 2007), the lower boundary of the altitude range considered in this study.

Adopting a common ion temperature of 250 K and a median electron temperature of 1000 K based on the RPWS LP measurements

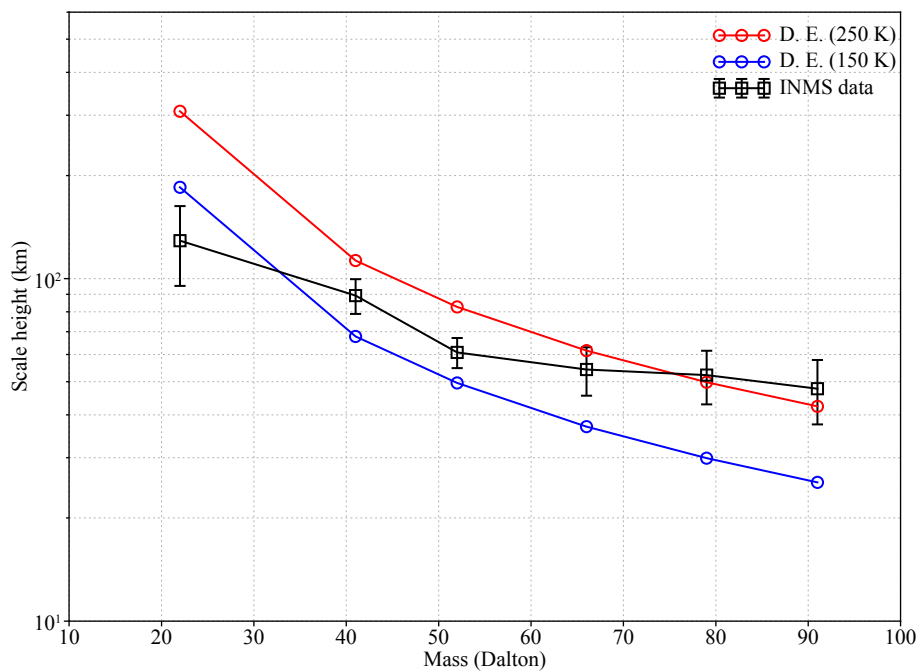


Figure 2. Comparison between the INMS scale heights (open squares) and the predicted scale heights under D. E. (open circles, red for an ion temperature of 250 K and blue for an ion temperature of 150 K) for the six ion groups investigated here.

at altitudes of our interest, equations (1) and (2) are combined to remove the electric field term which is then used to calculate the INMS ion density profile for G1 as a pseudo major ion species. The respective ion escape rate is treated as a free parameter in the data model comparison. The best-fit model profile is shown with the red line in Figure 3, giving an optimal ion escape rate of $(3.1 \pm 0.3) \times 10^{24} \text{ s}^{-1}$. For comparison, we show the D. E. solution for G1 with the dash-dotted line in the same figure. In general, the INMS data can be well reproduced by the simplified diffusion model except for the 50 km altitude range right above the lower boundary, as indicated by the red dashed line in the figure, which reflects model overestimate, presumably due to the neglect of chemistry for relatively light ion species approaching 1250 km. Existing studies reveal that the G1 ions such as CH_5^+ , C_2H_5^+ , and HCNH^+ suffer significant chemical loss both from reactions with ambient neutrals and from dissociative recombination with ambient electrons; with heavier ions (see below), the latter mechanism is dominant (e.g., Vuitton et al., 2007). We suggest that the disagreement between data and model for G1 approaching 1250 km is due to chemical processes occurring below that altitude that cannot be neglected. For instance, Cravens et al. (2009) showed that below 1300 km (see their Fig. 6) the chemical lifetimes of several species in the ion group G1, such as N_2^+ , CH_5^+ , C_2H_5^+ , and HCNH^+ , are less than the vertical and horizontal transport time.

Obtained in a similar manner, the best-fit diffusion models for ion mass groups G2 and G3 are shown with the red solid lines in Figures 4a and 4b, respectively, giving optimal escape rates of $(1.7 \pm 0.1) \times 10^{22} \text{ s}^{-1}$ for G2, and $(3.4 \pm 0.1) \times 10^{21} \text{ s}^{-1}$ for G3. The corresponding D. E. solutions are also shown with dash-dotted lines for comparison. The model fits observed data (not shown here) for the other ion mass groups—G4, G5, and G6, which are under D. E.,

as implied by Figure 2. Figure 4 also demonstrates that the diffusion model reasonably describes the INMS observations over the whole altitude range above 1250 km encountered here, thus validating our assumption of insignificant influence of ionospheric chemistry.

By adding together the derived escape rates for all ion groups, we obtain a total ion escape rate of $3.1 \times 10^{24} \text{ s}^{-1}$. According to our model results, relatively light ions with $M/Z < 32$ daltons account for more than 99% of total ion escape on Titan, with the remaining less than 1% supplied by the escape of heavier ions. A total ion mass escape rate of $114.8 \text{ g}\cdot\text{s}^{-1}$ is predicted from these results, of which only $1.2 \text{ g}\cdot\text{s}^{-1}$ is attributed to ions with M/Z from 36 to 45 Da, and $0.3 \text{ g}\cdot\text{s}^{-1}$ is attributed to ions with M/Z from 49 to 57 Da.

4. Concluding Remarks and Discussions

In this study, we investigate the relative contributions of different ion species to the total ion escape on Titan, by dividing all the ion species probed by the INMS into six groups according to their M/Z values. As compared to the observed density scale heights, the scale heights predicted by assuming D. E. are substantially greater for ion mass groups G1–G3 but in general agreement within measurement uncertainties for heavier groups G4–G6, implying that escaping ions on Titan are almost entirely contributed by relatively light species with $M/Z < 60$ daltons. We also construct a simplified diffusion model neglecting the effect of ionospheric chemistry, which is compared with the INMS data to constrain the ion escape rates for G1, G2, and G3. An optimal total ion escape rate of $3.1 \times 10^{24} \text{ s}^{-1}$ is obtained, of which more than 99% is contributed by G1. The corresponding total ion mass escape rate is $114.8 \text{ g}\cdot\text{s}^{-1}$.

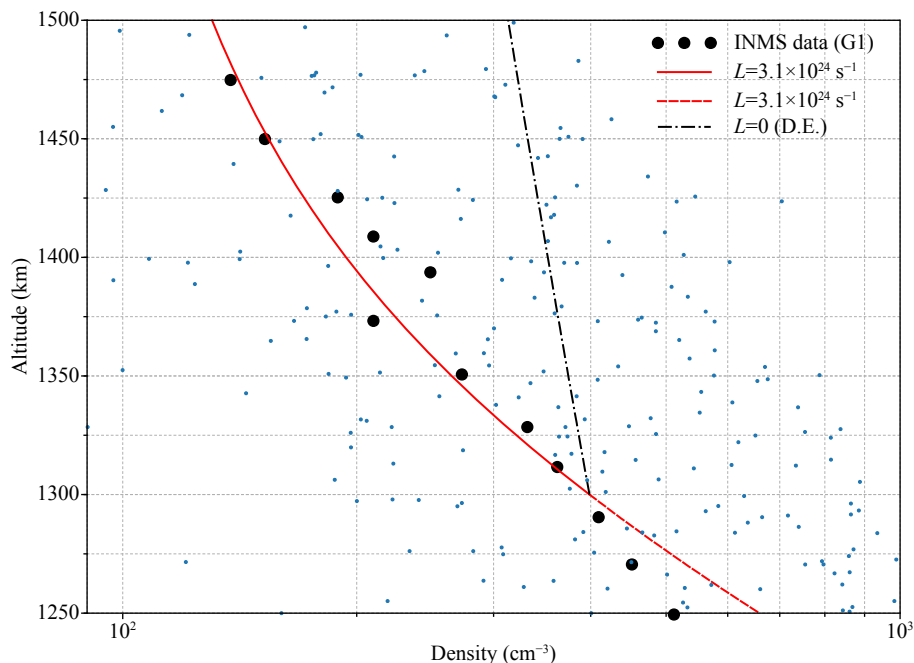


Figure 3. The globally averaged density profile of the ion mass group G1 as measured by the INMS, superimposed on the best-fit diffusion model given by the red solid line. The black dash-dotted line represents the profile under D. E. for comparison, which deviates substantially from the data. The red dashed line highlights the portion of Titan's ionosphere with clear data vs. model disagreement due to the neglect of chemical processes.

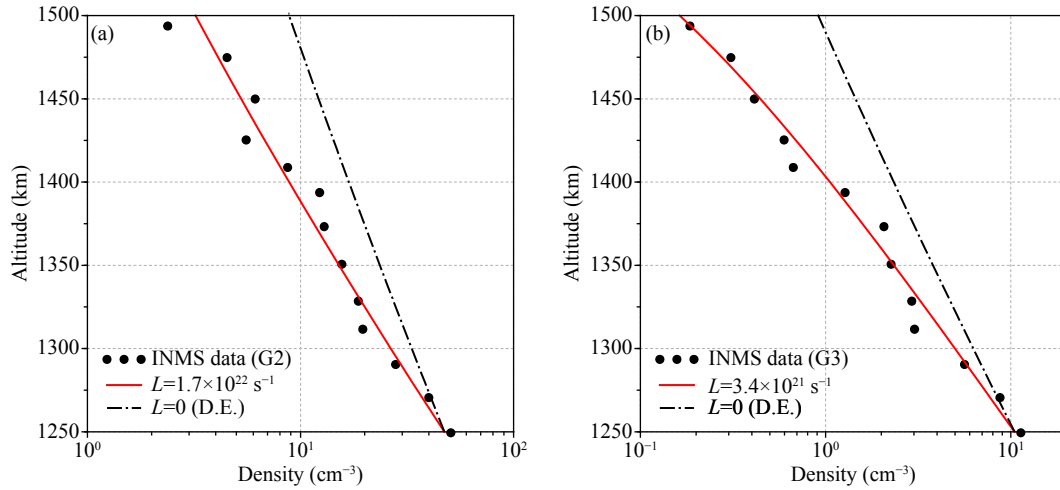


Figure 4. The global averaged density profiles for ion groups G2 (a) and G3 (b) measured by the INMS, superimposed on the best-fit diffusion models given by the red solid lines. The black dash-dotted lines represent the corresponding model profiles under D. E., which substantially disagree with the observations.

The ion escape rate given above is comparable to the result of $1.2 \times 10^{24} \text{ s}^{-1}$ inferred from Voyager 1 observations (Gurnett et al., 1982) and the result of $\sim(3\text{--}5) \times 10^{24} \text{ s}^{-1}$ predicted by MHD models (Ma YJ et al., 2006). However, our value is lower by an order of magnitude than the ion escape rate of $\sim 10^{25} \text{ s}^{-1}$ estimated by Wahlund et al. (2005) and Cui J et al. (2010) based on the electron distribution measured by the Cassini RPWS LP instrument, as well as the ion escape rate of $6 \times 10^{25} \text{ s}^{-1}$ predicted by the hybrid model calculations of Modolo and Chanteur (2008). Meanwhile, the hybrid simulation of Ledvina and Brecht (2012) incorporating negative ions in Titan's ionosphere (Coates et al., 2007, 2009) predicted a reduced loss rate by (5–20)% for light ions and an enhanced loss rate of (23–50)% for heavy ions, as compared to our results.

In this study, we adopt a constant electron temperature of 1000 K to simplify the calculations, but in reality, available RPWS/LP measurements reveal an increase in electron temperature from 1250 km to 1500 km (e.g., Wahlund et al., 2005; Edberg et al., 2010). To evaluate the impact of the adopted electron temperature on the modeling result, we calculate the escape rates with three representative electron temperature values of 800 K, 1000 K, and 1200 K; the computed escape rates are $[2.5, 3.1, \text{ and } 3.9] \times 10^{24} \text{ s}^{-1}$ for ion group G1, $[1.6, 1.7, \text{ and } 1.8] \times 10^{22} \text{ s}^{-1}$ for ion group G2, and $[3.3, 3.4, \text{ and } 3.5] \times 10^{21} \text{ s}^{-1}$ for ion group G3. These values imply that the uncertainty created by our adopted electron temperature has negligible effect on the computed escape rates of the heavier ion groups and only modestly affects the computed escape rate of G1 ions. The above distinction is clearly related to the dependence of the ambipolar electric field force on the electron temperature, and such a force is important only for relatively light ion species.

Momentum equations (1)–(3) are valid provided that the ion outflow is subsonic. Using the derived ion escape rates, the ion drift velocity for each ion group could be estimated to be $\sim(0.03\text{--}0.23) \text{ km}\cdot\text{s}^{-1}$ for G1, $\sim(0.002\text{--}0.04) \text{ km}\cdot\text{s}^{-1}$ for G2, and $\sim(0.002\text{--}0.1) \text{ km}\cdot\text{s}^{-1}$ for G3, all referred to the altitude range of 1250–1500 km. For comparison, the respective ion acoustic velocity ranges from 0.30

$\text{km}\cdot\text{s}^{-1}$ for G1 to $0.20 \text{ km}\cdot\text{s}^{-1}$ for G3. Therefore, the ion outflow indeed remains subsonic, validating use of the diffusion approximation in our calculations.

Our calculations indicate that the major and minor ions in Titan's ionosphere are accelerated upward by both the pressure gradient and the ambipolar electric field resulting from the separation between electrons and ions due to their mass difference (Coates et al., 2007). In addition, the major ions tend to drag the minor ions along with them via Coulomb interactions as they diffuse upward in response to the pressure gradient and the ambipolar field, as indicated by equation (3). Consequently, the relatively heavier minor ions belonging to groups G2 and G3 present an upward flow despite the fact that strong gravitational forces impede the motion of these ions.

Similar ion escape rates of $(10^{24}\text{--}10^{25}) \text{ s}^{-1}$ on other terrestrial planets such as Venus and Mars, despite great differences in their atmospheric/ionospheric properties and surrounding plasma environments, have been addressed in various studies (see Brain et al., 2016, and references therein). However, unlike Titan, on which a range of ion species experience significant escape, only one or two species dominate ion escape on both Mars (O^+) and Venus (O^+ , H^+) (Lundin, 2011). Detailed comparison of individual ion escape processes for these objects without global magnetic fields is required to address properly the coincidence in the ion loss rate.

Acknowledgments

We thank the two anonymous reviewers, whose constructive comments have significantly improved the quality of this paper. J. Cui acknowledges supports from the National Natural Science Foundation of China (NSFC) through grants 41525015 and 41774186. The data used in this study are available by the courtesy of the Cassini scientific teams.

References

Bird, M. K., Dutta-Roy, R., Asmar, S. W., and Rebold, T. A. (1997). Detection of Titan's ionosphere from voyager 1 radio occultation observations. *Icarus*,

- 130(2), 426–436. <https://doi.org/10.1006/icar.1997.5831>
- Brain, D. A., Bagenal, F., Ma, Y. J., Nilsson, H., and Stenberg Wieser, G. (2016). Atmospheric escape from unmagnetized bodies. *J. Geophys. Res. Planets*, 121(12), 2364–2385. <https://doi.org/10.1002/2016JE005162>
- Coates, A. J., Crary, F. J., Lewis, G. R., Young, D. T., Waite, J. H. Jr., and Sittler, E. C. Jr. (2007). Discovery of heavy negative ions in Titan's ionosphere. *Geophys. Res. Lett.*, 34(22), L22103. <https://doi.org/10.1029/2007GL030978>
- Coates, A. J., Wellbrock, A., Lewis, G. R., Jones, G. H., Young, D. T., Crary, F. J., and Waite, J. H. (2009). Heavy negative ions in Titan's ionosphere: altitude and latitude dependence. *Planet. Space Sci.*, 57(14–15), 1866–1871. <https://doi.org/10.1016/j.pss.2009.05.009>
- Coates, A. J., Wellbrock, A., Lewis, G. R., Arridge, C. S., Crary, F. J., Young, D. T., Thomsen, M. F., Reisenfeld, D. B., Sittler, E. C. Jr., ... Jones, G. H. (2012). Cassini in Titan's tail: CAPS observations of plasma escape. *J. Geophys. Res. Space Phys.*, 117(A5), A05324. <https://doi.org/10.1029/2012JA017595>
- Crary, F. J., Magee, B. A., Mandt, K., Waite, J. H., Westlake, J., and Young, D. T. (2009). Heavy ions, temperatures and winds in Titan's ionosphere: combined Cassini CAPS and INMS observations. *Planet. Space Sci.*, 57(14–15), 1847–1856. <https://doi.org/10.1016/j.pss.2009.09.006>
- Cravens, T. E., Robertson, I. P., Clark, J., Wahlund, J. E., Waite, J. H. Jr., Ledvina, S. A., Niemann, H. B., Yelle, R. V., Kasprzak, W. T., ... Coates, A. J. (2005). Titan's ionosphere: model comparisons with Cassini Ta data. *Geophys. Res. Lett.*, 32(12), L12108. <https://doi.org/10.1029/2005GL023249>
- Cravens, T. E., Robertson, I. P., Waite, J. H. Jr., Yelle, R. V., Kasprzak, W. T., Keller, C. N., Ledvina, S. A., Niemann, H. B., Luhmann, J. G., ... Vuitton, V. (2006). Composition of Titan's ionosphere. *Geophys. Res. Lett.*, 33(7), L07105. <https://doi.org/10.1029/2005GL025575>
- Cravens, T. E., Robertson, I. P., Waite, J. H. Jr., Yelle, R. V., Vuitton, V., Coates, A. J., Wahlund, J. E., Agren, K., Richard, R. K., ... Neubauer, F. M. (2009). Model-data comparisons for Titan's nightside ionosphere. *Icarus*, 199(1), 174–188. <https://doi.org/10.1016/j.icarus.2008.09.005>
- Cravens, T. E., Richard, R. K., Ma, Y. J., Bertucci, C., Luhmann, J. G., Ledvina, S., Robertson, I. P., Wahlund, J. E., Ågren, K., ... Ulusen, D. (2010). Dynamical and magnetic field time constants for Titan's ionosphere: empirical estimates and comparisons with Venus. *J. Geophys. Res.*, 115(A8), A08319. <https://doi.org/10.1029/2009JA015050>
- Cui, J., Yelle, R. V., and Volk, K. (2008). Distribution and escape of molecular hydrogen in Titan's thermosphere and exosphere. *J. Geophys. Res. Planets*, 113(E10), E10004. <https://doi.org/10.1029/2007JE003032>
- Cui, J., Galand, M., Yelle, R. V., Vuitton, V., Wahlund, J. E., Lavvas, P. P., Müller-Wodarg, I. C. F., Cravens, T. E., Kasprzak, W. T., and Waite, J. H. Jr. (2009). Diurnal variations of Titan's ionosphere. *J. Geophys. Res. Space Phys.*, 114(A6), A06310. <https://doi.org/10.1029/2009JA014228>
- Cui, J., Galand, M., Yelle, R. V., Wahlund, J. E., Ågren, K., Waite, J. H. Jr., and Dougherty, M. K. (2010). Ion transport in Titan's upper atmosphere. *J. Geophys. Res. Space Phys.*, 115(A6), A06314. <https://doi.org/10.1029/2009JA014563>
- Cui, J., Yelle, R. V., Müller-Wodarg, I. C. F., Lavvas, P. P., and Galand, M. (2011). The implications of the H₂ variability in Titan's exosphere. *J. Geophys. Res. Space Phys.*, 116(A11), A11324. <https://doi.org/10.1029/2011JA016808>
- De La Haye, V., Waite, J. H. Jr., Cravens, T. E., Nagy, A. F., Johnson, R. E., Lebonnois, S., and Robertson, I. P. (2007). Titan's corona: the contribution of exothermic chemistry. *Icarus*, 191(1), 236–250. <https://doi.org/10.1016/j.icarus.2007.04.031>
- Edberg, N. J. T., Wahlund, J. E., Ågren, K., Morooka, M. W., Modolo, R., Bertucci, C., and Dougherty, M. K. (2010). Electron density and temperature measurements in the cold plasma environment of Titan: implications for atmospheric escape. *Geophys. Res. Lett.*, 37(20), L20105. <https://doi.org/10.1029/2010GL044544>
- Gurnett, D. A., Scarf, F. L., and Kurth, W. S. (1982). The structure of Titan's wake from plasma wave observations. *J. Geophys. Res. Space Phys.*, 87(A3), 1395–1403. <https://doi.org/10.1029/JA087IA03p01395>
- Gurnett, D. A., Kurth, W. S., Kirchner, D. L., Hospodarsky, G. B., Averkamp, T. F., Zarka, P., Lecacheux, A., Manning, R., Roux, A., ... Pedersen, A. (2004). The Cassini radio and plasma wave investigation. *Space Sci. Rev.*, 114(1–4), 395–463. <https://doi.org/10.1007/s11214-004-1434-0>
- Ledvina, S. A., and Brecht, S. H. (2012). Consequences of negative ions for Titan's plasma interaction. *Geophys. Res. Lett.*, 39(20), L20103. <https://doi.org/10.1029/2012GL053835>
- Lundin, R. (2011). Ion acceleration and outflow from Mars and Venus: an overview. *Space Sci. Rev.*, 162(1–4), 309–334. <https://doi.org/10.1007/s11214-011-9811-y>
- Ma, Y. J., Nagy, A. F., Cravens, T. E., Sokolov, I. V., Hansen, K. C., Wahlund, J. E., Crary, F. J., Coates, A. J., and Dougherty, M. K. (2006). Comparisons between MHD model calculations and observations of Cassini flybys of Titan. *J. Geophys. Res. Space Phys.*, 111(A5), A05207. <https://doi.org/10.1029/2005JA011481>
- Mandt, K. E., Gell, D. A., Perry, M., Waite, J. K. Jr., Crary, F. A., Young, D., Magee, B. A., Westlake, J. H., Cravens, T., ... Liang, M. C. (2012). Ion densities and composition of Titan's upper atmosphere derived from the Cassini Ion Neutral Mass Spectrometer: analysis methods and comparison of measured ion densities to photochemical model simulations. *J. Geophys. Res. Planets*, 117(E10), E10006. <https://doi.org/10.1029/2012JE004139>
- Modolo, R., and Chanteur, G. M. (2008). A global hybrid model for Titan's interaction with the Kronian plasma: application to the Cassini Ta flyby. *J. Geophys. Res. Space Phys.*, 113(A1), A01317. <https://doi.org/10.1029/2007JA012453>
- Müller-Wodarg, I. C. F., Yelle, R. V., Cui, J., and Waite, J. H. (2008). Horizontal structures and dynamics of Titan's thermosphere. *J. Geophys. Res. Planets*, 113(E10), E10005. <https://doi.org/10.1029/2007JE003033>
- Romanelli, N., Modolo, R., Dubinin, E., Berthelier, J. J., Bertucci, C., Wahlund, J. E., Leblanc, F., Canu, P., Edberg, N. J. T., ... Dougherty, M. (2014). Outflow and plasma acceleration in Titan's induced magnetotail: evidence of magnetic tension forces. *J. Geophys. Res. Space Phys.*, 119(12), 9992–10005. <https://doi.org/10.1002/2014JA020391>
- Schunk, R. W., and Nagy, A. F. (2009). *Ionospheres: Physics, Plasma Physics, and Chemistry* (2nd ed). New York, USA: Cambridge University Press.
- Sillanpää, I., Kallio, E., Janhunen, P., Schmidt, W., Mursula, K., Vilppola, J., and Tanskanen, P. (2006). Hybrid simulation study of ion escape at Titan for different orbital positions. *Adv. Space Res.*, 38(4), 799–805. <https://doi.org/10.1016/j.asr.2006.01.005>
- Sittler, E. C. Jr., Hartle, R. E., Johnson, R. E., Cooper, J. F., Lipatov, A. S., Bertucci, C., Coates, A. J., Szego, K., Shappirio, M., ... Wahlund, J. E. (2010). Saturn's magnetospheric interaction with Titan as defined by Cassini encounters T9 and T18: new results. *Planet. Space Sci.*, 58(3), 327–350. <https://doi.org/10.1016/j.pss.2009.09.017>
- Strobel, D. F. (2010). Molecular hydrogen in Titan's atmosphere: implications of the measured tropospheric and thermospheric mole fractions. *Icarus*, 208(2), 878–886. <https://doi.org/10.1016/j.icarus.2010.03.003>
- Tucker, O. J., Johnson, R. E., Deighan, J. I., and Volkov, A. N. (2013). Diffusion and thermal escape of H₂ from Titan's atmosphere: Monte Carlo simulations. *Icarus*, 222(1), 149–158. <https://doi.org/10.1016/j.icarus.2012.10.016>
- Vuitton, V., Yelle, R. V., and McEwan, M. J. (2007). Ion chemistry and N-containing molecules in Titan's upper atmosphere. *Icarus*, 191(2), 722–742. <https://doi.org/10.1016/j.icarus.2007.06.023>
- Wahlund, J. E., Boström, R., Gustafsson, G., Gurnett, D. A., Kurth, W. S., Pedersen, A., Hospodarsky, G. B., Persoon, A. M., Canu, P., ... Müller-Wodarg, I. (2005). Cassini measurements of cold plasma in the ionosphere of Titan. *Science*, 308(5724), 986–989. <https://doi.org/10.1126/science.1109807>
- Wahlund, J. E., Galand, M., Müller-Wodarg, I., Cui, J., Yelle, R. V., Crary, F. J., Mandt, K., Magee, B., Waite, J. H. Jr., ... Kurth, W. S. (2009). On the amount of heavy molecular ions in Titan's ionosphere. *Planet. Space Sci.*, 57(14–15), 1857–1865. <https://doi.org/10.1016/j.pss.2009.07.014>
- Waite, J. H. Jr., Lewis, W. S., Kasprzak, W. T., Anicich, V. G., Block, B. P., Cravens, T. E., Fletcher, G. G., Ip, W. H., Luhmann, J. G., ... Yelle, R. V. (2004). The Cassini ion and neutral mass spectrometer (INMS) investigation. *Space Sci. Rev.*, 114(1–4), 113–231. <https://doi.org/10.1007/s11214-004-1408-2>
- Westlake, J. H., Paranicas, C. P., Cravens, T. E., Luhmann, J. G., Mandt, K. E., Smith, H. T., Mitchell, D. G., Rymer, A. M., Perry, M. E., ... Wahlund, J. E. (2012). The observed composition of ions outflowing from Titan. *Geophys. Res. Lett.*, 39(19), L19104. <https://doi.org/10.1029/2012GL053079>